2018 IEEE Intelligent Vehicles Symposium (IV)
Changshu, Suzhou, China, June 26-30, 2018

Fuzzy steering assistance control for path following of the steer-by-wire vehicle considering characteristics of human driver

Mengmeng Dai, Jinxiang Wang, Nan Chen, and Guodong Yin

Abstract—**The fuzzy full-order dynamic output-feedback steering assistance control is proposed in this paper to follow large-curvature path for the steer-by-wire (SBW) vehicle. The driver-vehicle-road (DVR) model to follow large-curvature path is built under the assumption that the near and far vision information of the road for guidance is considered by the human driver. Five parameters describing the driver's steering characteristics and behaviors are considered as uncertainties of the DVR models with different drivers. The Takagi-Sugeno (T-S) fuzzy model is applied to handle these uncertainties in designing the dynamic output-feedback parallel distributed compensator (DPDC). The compensator design is then reduced to solving several linear matrix inequalities (LMIs). Simulation results show that the proposed controller can provide different human drivers with individual steering assistance in following the large-curvature path, and can reduce the driver's physical and mental workloads.**

I. INTRODUCTION

Among various kinds of advanced driver-assistance systems (ADAS), steering assistance system is one of the most promising approaches contributing to improvement of vehicle's maneuverability, safety, and driving comfort [1][2]. The steer-by-wire (SBW) system has been considered as the next generation steering system equipped on the ground vehicles for the improvement of overall steering performance [3]. Since the mechanical linkage between the driver's hand wheel and the steering wheels is removed, the SBW system enables the automation system to exert an automatic steering assistance more conventionally and readily by augmenting driver's steering commands, which is regarded as the most valuable advantage of the SBW[4][5].

For the ADAS, if the steering assistance system is designed with consideration of the human drivers' characteristics, it can provide more personalized steering assistance. Since different drivers have different driving propensities, and even behave dissimilarly under the identical maneuver, the human driver's driving behaviors are essential for designing the steering assistance controller to assist different drivers better. Generally, the driver's preview action, delay behavior, and steering behavior in path following can be considered and parameterized to describe a driver's driving characteristics [6][7].

The Takagi-Sugeno (T-S) fuzzy control is effective to deal with the parameter uncertainties for an underlying nonlinear system. Based on the idea of sector nonlinearity and a set of fuzzy *IF-THEN* rules for describing the local linear representation, a nonlinear system can be approximated as a weighted sum of some simple linear subsystems. Thanks to the transformation of polytopic framework of linear subsystems, the T-S fuzzy model can be analyzed and optimized though the linear system theories. Owing to its merit in handling uncertainties, the T-S fuzzy control has been widely applied in system stability analysis and controller synthesis [8][9][10][11].

In this paper, a two-point preview control strategy using both near and far region information of the road is presented for describing a two-level driver model incorporating the driver's anticipatory and compensatory actions. By applying the two-point preview control, a large-curvature path can be followed, which cannot be achieved via the single-point preview control [12][13]. Based on this driver model, the fuzzy dynamic output-feedback control is employed to allow both the human diver and the automation being able to appropriately share the authority to control the steering wheels. This proposed shared controller can provide continuous and individual assistance for different human drivers. And with the proposed fuzzy dynamic output-feedback controller, not only the cost in sensors can be cut down, but the pole placement can be introduced to improve the performance of the closed-loop system, which is NP-hard in static output-feedback control [14].

The main contributions of this paper are as follows: 1) the two-level driver model is proposed to follow the large-curvature path, with which the characteristics of driver's steering behavior are considered, including the anticipation steering gain, compensation steering gain, derivative time, preview time, and delay time. 2) A linear parameter-varying DVR model is built based on the T-S fuzzy model. 3) Regional pole placement based on the quadratic *D*-stability is introduced in the dynamic output-feedback control to improve performance of the closed-loop DVR system, and the sufficient conditions are derived with respect to a set of linear matrix inequalities (LMIs).

Notation: $\boldsymbol{0}$ and $\boldsymbol{I}$ are used to represent zero matrix and identify matrix of appropriate dimensions. $\|\cdot\|_2$ is used to denote the L_2-norm of a matrix. For a real symmetric matrix $\boldsymbol{P}$, $\boldsymbol{P} \prec 0$ ($\boldsymbol{P} \succ 0$) denotes its negative (positive) definiteness. In a symmetric block matrix, $*$ is used as an ellipsis for terms that can be readily obtained by symmetry.

II. DRIVER-VEHICLE-ROAD MODELING

A. Vehicle-Road Model

The vehicle-road model of path following is based on the two-point preview model with both near and far region information of the road [15]. As shown in Fig.1, a near point is utilized to maintain the vehicle along centerline of the lane by minimizing θ_{near} between the vehicle heading and the line directing toward the near point, or alternatively minimizing

This research is partially supported by National Natural Science Foundation of China (NSFC) under Grant 51675099, U1664258, and 51575103, and the Fundamental Research Funds for the Central Universities under Grant 2242017K40197. All correspondence should be sent to J. Wang (Email: wangjx@seu.edu.cn).

The authors are with the School of Mechanical Engineering, Southeast University, Nanjing, 211189, China.

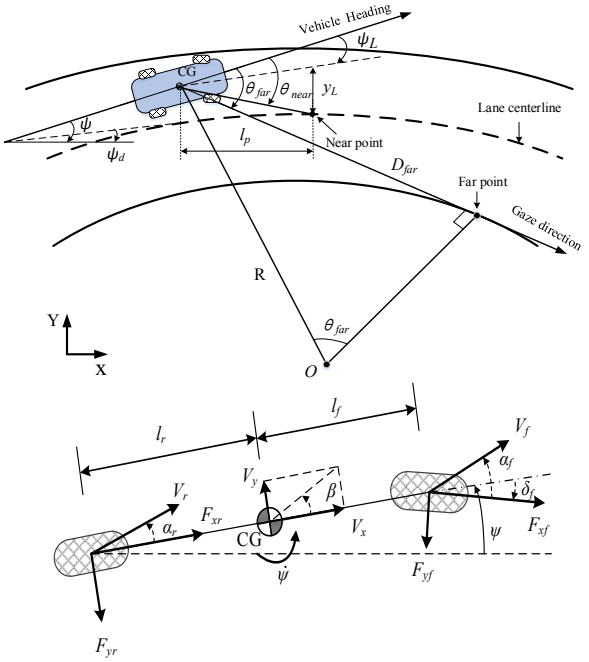

Fig.1 Two-point preview path following model and the bicycle model

the heading error ψ_L and the lateral deviation y_L. A far point is utilized to account for the upcoming road, through which the road curvature can be obtained. Besides, note that the far point is selected as the tangent point of the inside lane edge, as the drivers spend average 72.2% time gazing at the region of 5 degree around the tangent point when negotiating the curve [16]. The vehicle-road model can be described as

$$\dot{\boldsymbol{x}}_v = \boldsymbol{A}_v \boldsymbol{x}_v + \boldsymbol{B}_{v1}\delta_f + \boldsymbol{B}_{v2}\omega + \hat{\boldsymbol{d}} \ , \tag{1}$$

where $\boldsymbol{A}_v = \begin{bmatrix} a_{11} & a_{12} & 0 & 0 \\ a_{21} & a_{22} & 0 & 0 \\ 0 & 1 & 0 & 0 \\ 1 & l_p & V_x & 0 \end{bmatrix}$, $\boldsymbol{B}_{v1} = \begin{bmatrix} b_1 \\ b_2 \\ 0 \\ 0 \end{bmatrix}$, $\boldsymbol{B}_{v2} = \begin{bmatrix} 0 \\ 0 \\ -V_x \\ -l_p V_x \end{bmatrix}$,

$a_{11} = \dfrac{-2(C_f + C_r)}{m V_x}$, $a_{12} = -V_x + \dfrac{2(C_r l_r - C_f l_f)}{m V_x}$, $b_1 = \dfrac{2C_f}{m}$,

$a_{21} = \dfrac{2(C_r l_r - C_f l_f)}{I_z V_x}$, $a_{22} = \dfrac{-2(C_f l_f^2 + C_r l_r^2)}{I_z V_x}$, $b_2 = \dfrac{2C_f l_f}{I_z}$.

The state vector $\boldsymbol{x}_v = [V_y \ \ r \ \ \psi_L \ \ y_L]^T$ comprises the lateral speed V_y, yaw rate r, heading error ψ_L, and the lateral offset y_L between the vehicle and the desired lane centerline at the near point. The disturbance input $\omega = \rho_r$, and the modeling error $\hat{\boldsymbol{d}} = [d_1 \ \ d_2 \ \ d_3 \ \ d_4]^T$. Other parameters of the vehicle-road model can be found in Table I.

B. Driver Model

It is assumed that the driver considers near and far vision information of the road for guidance, which can be represented by the angles between the vehicle heading and the lines directing toward the two preview points, i.e. θ_{far} and θ_{near} (see Fig.1). Actually, θ_{far} and θ_{near} describe the driver's motivations of feedforward and feedback steering control, respectively, and can be calculated as

$$\theta_{near} = \frac{y_L}{l_p} + \psi_L, \ \theta_{far} \approx \frac{D_{far}}{R} = D_{far}\rho_r. \tag{2}$$

TABLE I. PARAMETERS OF THE VEHICLE-ROAD MODEL

Symbol	Meaning	Value
m	Vehicle total mass	1705 kg
I_z	Vehicle yaw moment of inertia	3048 kg.m^2
l_f	Distance between CG and front axle	1.035 m
l_r	Distance between CG and rear axle	1.665 m
C_f	Equivalent Cornering Stiffness of front tire	103130N/rad
C_r	Equivalent Cornering Stiffness of rear tire	73854 N/rad
ρ_r	Road curvature	--
l_p	Preview distance between CG and near point	--
D_{far}	Preview distance between CG and far point	--
R	Distance between CG and the turning center	--

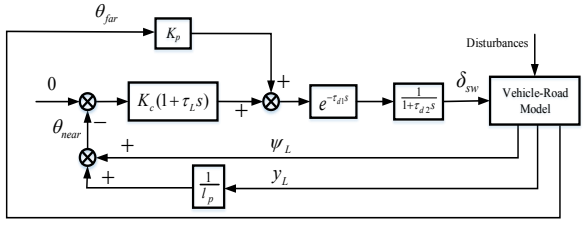

Fig.2 The structure of driver model

As depicted in Fig. 2, there are two levels for the driver model. The upper-level represents the driver's feedforward steering control, where K_p is the anticipatory steering gain to compensate the road curvature. The lower-level represents the driver's feedback steering control to minimize the error of near-point visual angle, where the desired θ_{near} is zero. The feedback steering control is realized by the PD controller, in which coefficients K_c and τ_L are the compensation steering gain and derivative time constant, respectively. Sum of the feedforward and feedback control outputs is formulated as the driver's steering intention. $e^{-\tau_{d1}s}$ describes the driver's brain response delay, and $\frac{1}{1+\tau_{d2}s}$ describes the delay of neuromuscular system of the driver's arms.

According to Fig.2, the steering angle $\delta_{sw}(s)$ exerted on the steering wheel by the driver can be represented as

$$\delta_{sw}(s) = \frac{e^{-\tau_{d1}s}}{1+\tau_{d2}s}\left[K_p\theta_{far}(s) - K_c(1+\tau_L s)\theta_{near}(s)\right]. \tag{3}$$

Note that the pure time delay $e^{-\tau_{d1}s}$ can be expanded by Taylor Formula and then approximated by a first-order lag element as $\frac{1}{1+\tau_{d1}s}$. By assuming the steering ratio to be R_g, the driver's portion of front wheel steering angle is $\delta_{fd} = R_g\delta_{sw}$. Therefore the driver model can be rewritten as

$$\begin{aligned}\delta_{fd} = \int[-\frac{1}{a_0 T_d}\delta_{fd} - \frac{R_g K_c \tau_L}{a_0 T_d}\theta_{near} + \int(-\frac{1}{a_0 T_d^2}\delta_{fd} + \\ \frac{R_g K_p}{a_0 T_d^2}\theta_{far} - \frac{R_g K_c}{a_0 T_d^2}\theta_{near})dt]\,dt + d',\end{aligned} \tag{4}$$

where $T_d = \tau_{d1} + \tau_{d2}$ is the delay time, and $a_0 = \tau_{d1}\tau_{d2}/T_d^2$. We fix a_0 as a constant for the sake of controller design [13]. d' is the modeling error due to the approximations.

With above approximations, the state-space driver model can be derived from (4) and described as

$$\begin{bmatrix} \dot{x}_1 \\ \dot{\delta}_{fd} \end{bmatrix} = \begin{bmatrix} 0 & \frac{-1}{a_0 T_d^2} \\ 1 & \frac{-1}{a_0 T_d} \end{bmatrix}\begin{bmatrix} x_1 \\ \delta_{fd} \end{bmatrix} + \begin{bmatrix} -\frac{R_g K_c}{a_0 T_d^2} & \frac{R_g K_p}{a_0 T_d^2} \\ -\frac{R_g K_c \tau_L}{a_0 T_d^2} & 0 \end{bmatrix}\begin{bmatrix} \theta_{near} \\ \theta_{far} \end{bmatrix} + \begin{bmatrix} d_5 \\ d_6 \end{bmatrix}. \tag{5}$$

where $x_1 = \int (-\frac{1}{a_0 T_d^{\,2}}\delta_{fd} + \frac{R_g K_p}{a_0 T_d^{\,2}}\theta_{far} - \frac{R_g K_c}{a_0 T_d^{\,2}}\theta_{near})dt$.

Remark 1. θ_{near} and θ_{far} are the inputs of the driver model (5). It is assumed that the two preview distances have the relationship of $l_p = 0.4 D_{far}$. The preview time T_p is defined as

$$T_p = \frac{D_{far}}{V_x}. \tag{6}$$

Then in (5) the characteristics of different human drivers can be determined by uncertain parameters described as $\boldsymbol{\pi} = [K_p \quad K_c \quad \tau_L \quad T_d \quad T_p]^T$. The behaviors of a typical driver can be captured after $\boldsymbol{\pi}$ is identified.

Remark 2. As for identification of the driver's characteristic vector $\boldsymbol{\pi}$, a feasible solution is to treat the state-space driver model (5) as a grey box [17]. By using the prediction error method, the characteristic parameters that lead to the smallest L_2-*norm* of the prediction error of δ_{fd} can be obtained. The identification approach can be achieved by using the *System Identification Toolbox* in Matlab.

III. T-S FUZZY MODELING OF DVR SYSTEM

By combining (1), (2), (5), and (6), the controlled DVR model can be obtained as

$$\dot{\boldsymbol{x}} = \boldsymbol{A}\boldsymbol{x} + \boldsymbol{B}_u u + \boldsymbol{B}_w \omega + \boldsymbol{d}\ , \tag{7}$$

where $\boldsymbol{x} = \begin{bmatrix} V_y & r & \psi_L & y_L & x_1 & \delta_{fd} \end{bmatrix}^T$, $u=\delta_{fc}$, $\omega=\rho_r$,

$$\boldsymbol{A} = \begin{bmatrix} \boldsymbol{A}_{11} & \boldsymbol{A}_{12} \\ \boldsymbol{A}_{21} & \boldsymbol{A}_{22} \end{bmatrix},\ \boldsymbol{A}_{11} = \boldsymbol{A}_v,\ \boldsymbol{A}_{12} = [\boldsymbol{0} \quad \boldsymbol{B}_{v1}],\ \boldsymbol{B}_u = \begin{bmatrix} \boldsymbol{B}_{v1}^{\ T} & \boldsymbol{0} \end{bmatrix}^T,$$

$$\boldsymbol{A}_{21} = \begin{bmatrix} 0 & 0 & -\frac{R_g K_c}{a_0 T_d^{\,2}} & -\frac{2.5 R_g K_c}{a_0 V_x T_p T_d^{\,2}} \\ 0 & 0 & -\frac{R_g K_c \tau_L}{a_0 T_d^{\,2}} & -\frac{2.5 R_g K_c \tau_L}{a_0 V_x T_p T_d^{\,2}} \end{bmatrix},\ \boldsymbol{A}_{22} = \begin{bmatrix} 0 & -\frac{1}{a_0 T_d^{\,2}} \\ 1 & -\frac{1}{a_0 T_d} \end{bmatrix},$$

$$\boldsymbol{B}_w = \begin{bmatrix} 0 & 0 & -V_x & -0.4 V_x^{\,2} T_p & \frac{R_g K_p T_p V_x}{a_0 T_d^{\,2}} & 0 \end{bmatrix}^T,\ \boldsymbol{d} = \begin{bmatrix} d_1 & d_2 & d_3 & d_4 & d_5 & d_6 \end{bmatrix}^T.$$

Note that V_y is expensively measureable from the viewpoint of application. To this end, for sensor cost reduction, we only consider the rest states as the measured outputs, and yield

$$\boldsymbol{y} = \boldsymbol{C}_y \boldsymbol{x}\ , \tag{8}$$

where $\boldsymbol{C}_y = [\boldsymbol{0} \quad \boldsymbol{I}]$.

For improving the performance of path following, the heading error ψ_L and lateral deviation y_L should be as small as possible, and for the sake of enhancing vehicle handling stability, V_y should not be large. Furthermore, by considering that the driver's physical and mental workloads should also be decreased by the steering assistance system, δ_{fd} and $\dot{\delta}_{fd}$ should be taken as the performance outputs [12][13]. As a consequence, a performance output vector including the performances of both path following and driver's comfort is defined as

$$\boldsymbol{z} = \boldsymbol{C}_z \boldsymbol{x} = \begin{bmatrix} V_y & \psi_L & y_L & \delta_{fd} & \dot{\delta}_{fd} \end{bmatrix}^T. \tag{9}$$

Finally, the path-following DVR plant is obtained as

$$\begin{cases} \dot{\boldsymbol{x}} = \boldsymbol{A}\boldsymbol{x} + \boldsymbol{B}_u u + \boldsymbol{B}_w w + \boldsymbol{d} \\ \boldsymbol{z} = \boldsymbol{C}_z \boldsymbol{x} \\ \boldsymbol{y} = \boldsymbol{C}_y \boldsymbol{x} \end{cases} \tag{10}$$

TABLE II. LIST OF FUZZY RULES

Rule No.	Premise variables					Rule No.	Premise variables				
	K_p	K_c	τ_L	T_d	T_p		K_p	K_c	τ_L	T_d	T_p
1	S	S	S	S	S	17	B	S	S	S	S
2	S	S	S	S	B	18	B	S	S	S	B
3	S	S	S	B	S	19	B	S	S	B	S
4	S	S	S	B	B	20	B	S	S	B	B
5	S	S	B	S	S	21	B	S	B	S	S
6	S	S	B	S	B	22	B	S	B	S	B
7	S	S	B	B	S	23	B	S	B	B	S
8	S	S	B	B	B	24	B	S	B	B	B
9	S	B	S	S	S	25	B	B	S	S	S
10	S	B	S	S	B	26	B	B	S	S	B
11	S	B	S	B	S	27	B	B	S	B	S
12	S	B	S	B	B	28	B	B	S	B	B
13	S	B	B	S	S	29	B	B	B	S	S
14	S	B	B	S	B	30	B	B	B	S	B
15	S	B	B	B	S	31	B	B	B	B	S
16	S	B	B	B	B	32	B	B	B	B	B

Since there exist five uncertain parameters describing different human driver's characteristics in $\boldsymbol{A}$, $\boldsymbol{B}_w$, and $\boldsymbol{C}_z$, the DVR model (10) is actually nonlinear. The T-S fuzzy approach is applied to handle this challenging problem. By regarding each parameter $\pi_i (i = 1, 2, ..., 5)$ as a premise variable, and by assuming that π_i is bounded in practice as $\pi_{i\min} \le \pi_i \le \pi_{i\max}$, then based on the idea of sector nonlinearity, each premise variable π_i can be represented as

$$\pi_i = \lambda_{1i}(\pi_i)\pi_{i\min} + \lambda_{2i}(\pi_i)\pi_{i\max}, \tag{11}$$

where $\lambda_{1i}(\pi_i)$, $\lambda_{2i}(\pi_i)$ are the membership function satisfying $\lambda_{1i}(\pi_i) + \lambda_{2i}(\pi_i) = 1$, calculated as

$$\lambda_{1i}(\pi_i) = \frac{\pi_{i\max} - \pi_i}{\pi_{i\max} - \pi_{i\min}},\ \lambda_{2i}(\pi_i) = \frac{\pi_i - \pi_{i\min}}{\pi_{i\max} - \pi_{i\min}}\ . \tag{12}$$

As a consequence, the nonlinear DVR model (10) is further linearized with a T-S fuzzy model including 2^5 fuzzy rules, as can be found in Table II, where B and S represent *big* and *small* respectively. In order to describe the T-S fuzzy model more clearly, an example of the fuzzy *IF-THEN* rules listed in Table II is explained as follows.

Model Rule 1:

IF K_P is small, K_c is small, τ_L is small, T_d is small, and T_p is small, *THEN* the open-loop DVR system is

$$\begin{cases} \dot{\boldsymbol{x}} = \boldsymbol{A}_1 \boldsymbol{x} + \boldsymbol{B}_u u + \boldsymbol{B}_{w1} \omega + \boldsymbol{d}_1 \\ \boldsymbol{z} = \boldsymbol{C}_{z1} \boldsymbol{x} \\ \boldsymbol{y} = \boldsymbol{C}_y \boldsymbol{x} \end{cases}.$$

Matrices $\boldsymbol{A}_1$, $\boldsymbol{B}_{w1}$, and $\boldsymbol{C}_{z1}$ are obtained by replacing K_P, K_c, τ_L, T_d, and T_p in matrices $\boldsymbol{A}$, $\boldsymbol{B}_w$, and $\boldsymbol{C}_z$ with $K_{P\min}$, $K_{c\min}$, $\tau_{L\min}$, $T_{d\min}$, and T_{pmin}, respectively.

Finally, the T-S fuzzy model of DVR system under the assumption of $\pi_i \in [\pi_{i\min} \quad \pi_{i\max}]$ can be represented as

$$\begin{cases} \dot{\boldsymbol{x}} = \sum_{i=1}^{32} h_i(\pi)(\boldsymbol{A}_i \boldsymbol{x} + \boldsymbol{B}_{wi}\omega + \boldsymbol{d}_i) + \boldsymbol{B}_u u \\ \boldsymbol{z} = \sum_{i=1}^{32} h_i(\pi)\boldsymbol{C}_{zi}\boldsymbol{x} \\ \boldsymbol{y} = \boldsymbol{C}_y \boldsymbol{x} \end{cases} \tag{13}$$

where the weighting function $h_i(\pi)$ satisfies

$$\sum_{i=1}^{32} h_i(\pi) = 1,\quad h_i(\pi) > 0, i = 1, 2, ..., 32\ ,$$

and is represented as

$$\begin{cases} h_1(\pi) = \lambda_{11}(\pi_1) \times \lambda_{12}(\pi_2) \times \lambda_{13}(\pi_3) \times \lambda_{14}(\pi_4) \times \lambda_{15}(\pi_5) \\ h_2(\pi) = \lambda_{11}(\pi_1) \times \lambda_{12}(\pi_2) \times \lambda_{13}(\pi_3) \times \lambda_{14}(\pi_4) \times \lambda_{25}(\pi_5) \\ h_3(\pi) = \lambda_{11}(\pi_1) \times \lambda_{12}(\pi_2) \times \lambda_{13}(\pi_3) \times \lambda_{24}(\pi_4) \times \lambda_{15}(\pi_5) \\ h_4(\pi) = \lambda_{11}(\pi_1) \times \lambda_{12}(\pi_2) \times \lambda_{13}(\pi_3) \times \lambda_{24}(\pi_4) \times \lambda_{25}(\pi_5) \\ \vdots \\ h_{32}(\pi) = \lambda_{21}(\pi_1) \times \lambda_{22}(\pi_2) \times \lambda_{23}(\pi_3) \times \lambda_{24}(\pi_4) \times \lambda_{25}(\pi_5) \end{cases} \quad (14)$$

IV. FUZZY DYNAMIC OUTPUT-FEEDBACK CONTROLLER DESIGN

A. Fuzzy full-order dynamic output-feedback control law

In order to design the LMI-based fuzzy full-order dynamic compensator, the concept of DPDC is introduced. In DPDC, each control rule is designed according to the corresponding rule of the T-S fuzzy model, and the designed fuzzy dynamic compensator shares the same fuzzy sets with the fuzzy model [18]. For a given T-S fuzzy model, the DPDC usually has linear, quadratic, and cubic methods of parameterization, and the choice of a particular method of parameterization is determined by the structure of the T-S subsystems. Since each subsystem of the T-S fuzzy DVR system (13) has identical B_u and C_y, i.e., B_u=B_{ui} and C_y=C_{yi} (i=1, 2, … , 32), the compensator to be designed has a linear parameterization in the following form:

Dynamic Part: Rule i

IF the open-loop DVR system is

$$\begin{cases} \dot{\boldsymbol{x}} = \boldsymbol{A}_i \boldsymbol{x} + \boldsymbol{B}_u u + \boldsymbol{B}_{wi} w + \boldsymbol{d}_i \\ \boldsymbol{z} = \boldsymbol{C}_{zi} \boldsymbol{x} \\ \boldsymbol{y} = \boldsymbol{C}_y \boldsymbol{x} \end{cases} \quad (15)$$

THEN $\dot{\boldsymbol{x}}_c = \boldsymbol{A}_{ci} \boldsymbol{x}_c + \boldsymbol{B}_{ci} y$.

Output Part: Rule i

IF the open-loop DVR system is (15), *THEN* $\boldsymbol{u} = \boldsymbol{C}_{ci} \boldsymbol{x}_c + \boldsymbol{D}_{ci} \boldsymbol{y}$.

As a result, the DPDC compensator is written as

$$\begin{cases} \dot{\boldsymbol{x}}_c = \sum_{i=1}^{32} h_i(\pi)(\boldsymbol{A}_{ci} \boldsymbol{x}_c + \boldsymbol{B}_{ci} \boldsymbol{y}) \\ \boldsymbol{u} = \sum_{i=1}^{32} h_i(\pi)(\boldsymbol{C}_{ci} \boldsymbol{x}_c + \boldsymbol{D}_{ci} \boldsymbol{y}) \end{cases} \quad (16)$$

where $\boldsymbol{A}_{ci} \in \Re^{6\times6}$, $\boldsymbol{B}_{ci} \in \Re^{6\times5}$, $\boldsymbol{C}_{ci} \in \Re^{1\times6}$, and $\boldsymbol{D}_{ci} \in \Re^{1\times5}$ (i=1, 2, … , 32) are the gain matrices to be designed. By combining (13) and (16), the fuzzy closed-loop DVR model is obtained as

$$\begin{cases} \dot{\boldsymbol{x}}_{cl} = \sum_{i=1}^{32} h_i(\pi)(\boldsymbol{A}_{cli} \boldsymbol{x}_{cl} + \boldsymbol{B}_{cwi} \omega + \boldsymbol{B}_{cd} \hat{\boldsymbol{d}}_i) \\ z = \sum_{i=1}^{32} h_i(\pi) \boldsymbol{C}_{cli} \boldsymbol{x}_{cl} \end{cases}, \quad (17)$$

with $\boldsymbol{x}_{cl} = \begin{bmatrix} \boldsymbol{x} \\ \boldsymbol{x}_c \end{bmatrix}$, $\boldsymbol{A}_{cli} = \begin{bmatrix} \boldsymbol{A}_i + \boldsymbol{B}_u \boldsymbol{D}_{ci} \boldsymbol{C}_y & \boldsymbol{B}_u \boldsymbol{C}_{ci} \\ \boldsymbol{B}_{ci} \boldsymbol{C}_y & \boldsymbol{A}_{ci} \end{bmatrix}$, $\boldsymbol{B}_{cwi} = \begin{bmatrix} \boldsymbol{B}_{wi} \\ \boldsymbol{0} \end{bmatrix}$,

$\boldsymbol{B}_{cd} = [\boldsymbol{I} \quad \boldsymbol{0}]^T$, $\hat{\boldsymbol{d}}_i = \boldsymbol{d}_i$, $\boldsymbol{C}_{cli} = [\boldsymbol{C}_{zi} \quad \boldsymbol{0}]$.

The goal is to design a fuzzy full-order dynamic compensator that makes model (17) globally quadratically stabilizable. And with this compensator the effects of disturbance ω and $\hat{\boldsymbol{d}}$ to the control output $\boldsymbol{z}$ should be attenuated to a prescribed level in the presence of parameter uncertainties. Therefore the H_∞ performances are chosen as

$$\|z\|_2 < \kappa_1 \|\omega\|_2, \ \|z\|_2 < \kappa_2 \|\hat{\boldsymbol{d}}\|_2, \quad (18)$$

where $\kappa_1, \kappa_2 > 0$ are the prescribed attenuation level.

Now we are in the position to propose the fuzzy full-order dynamic output-feedback control law, and the following theorem is introduced.

Theorem 1 [11]. The fuzzy closed-loop DVR system (17) is globally stabilizable, and the H_∞ performance (18) holds, if and only if there exist symmetric positive definite matrices $\boldsymbol{X} \in \Re^{6\times6}$, $\boldsymbol{Y} \in \Re^{6\times6}$, and matrices $\hat{\boldsymbol{A}}_i \in \Re^{6\times6}$, $\hat{\boldsymbol{B}}_i \in \Re^{6\times5}$, $\hat{\boldsymbol{C}}_i \in \Re^{1\times6}$, $\hat{\boldsymbol{D}}_i \in \Re^{1\times5}$ (i=1,2,…,32) satisfying

$$\begin{bmatrix} \varphi_{11}(i) & \varphi_{12}(i) & \boldsymbol{B}_{wi}^T & \boldsymbol{X}\boldsymbol{C}_{zi}^T \\ * & \varphi_{22}(i) & \boldsymbol{Y}\boldsymbol{B}_{wi} & \boldsymbol{C}_{zi}^T \\ * & * & -\kappa_1 \boldsymbol{I} & \boldsymbol{0} \\ * & * & * & -\kappa_1 \boldsymbol{I} \end{bmatrix} \prec 0 \quad (19)$$

$$\begin{bmatrix} \varphi_{11}(i) & \varphi_{12}(i) & \boldsymbol{I} & \boldsymbol{X}\boldsymbol{C}_{zi}^T \\ * & \varphi_{22}(i) & \boldsymbol{Y} & \boldsymbol{C}_{zi}^T \\ * & * & -\kappa_2 \boldsymbol{I} & \boldsymbol{0} \\ * & * & * & -\kappa_2 \boldsymbol{I} \end{bmatrix} \prec 0 \quad (20)$$

with

$$\begin{aligned} \varphi_{11}(i) &= \boldsymbol{A}_i \boldsymbol{X} + \boldsymbol{X}\boldsymbol{A}_i^T + \boldsymbol{B}_u \hat{\boldsymbol{C}}_i + (\boldsymbol{B}_u \hat{\boldsymbol{C}}_i)^T \\ \varphi_{12}(i) &= \hat{\boldsymbol{A}}_i^T + \boldsymbol{A}_i + \boldsymbol{B}_u \hat{\boldsymbol{D}}_i \boldsymbol{C}_y \\ \varphi_{22}(i) &= \boldsymbol{A}_i^T \boldsymbol{Y} + \boldsymbol{Y}\boldsymbol{A}_i + \hat{\boldsymbol{B}}_i \boldsymbol{C}_y + (\hat{\boldsymbol{B}}_i \boldsymbol{C}_y)^T \end{aligned}$$

Furthermore, the gain matrices for each fuzzy submodel in (16) are calculated as

$$\begin{cases} \boldsymbol{D}_{ci} = \hat{\boldsymbol{D}}_i, \\ \boldsymbol{C}_{ci} = \left(\hat{\boldsymbol{C}}_i - \boldsymbol{D}_{ci} \boldsymbol{C}_y \boldsymbol{X}\right)(\boldsymbol{M}^T)^{-1}, \\ \boldsymbol{B}_{ci} = \boldsymbol{N}^{-1}\left(\hat{\boldsymbol{B}}_i - \boldsymbol{Y}\boldsymbol{B}_u \boldsymbol{D}_{ci}\right), \\ \boldsymbol{A}_{ci} = \boldsymbol{N}^{-1}\left[\hat{\boldsymbol{A}}_i - \boldsymbol{Y}\left(\boldsymbol{A}_i + \boldsymbol{B}_u \boldsymbol{D}_{ci} \boldsymbol{C}_y\right)\boldsymbol{X}\right](\boldsymbol{M}^T)^{-1} \\ \qquad - \boldsymbol{B}_{ci} \boldsymbol{C}_y \boldsymbol{X}(\boldsymbol{M}^T)^{-1} - \boldsymbol{N}^{-1} \boldsymbol{Y} \boldsymbol{B}_u \boldsymbol{C}_{ci} \end{cases} \quad (21)$$

where full-rank matrices $\boldsymbol{M}$ and $\boldsymbol{N}$ satisfy $\boldsymbol{M}\boldsymbol{N}^T = \boldsymbol{I} - \boldsymbol{X}\boldsymbol{Y}$, and can be obtained by the *QR* function in Matlab.

B. Regional pole placement

It is well-known that pole clustering in the left-half complex plane can only guarantee stabilization of the system, not qualified for the requirement of transient performance. To achieve satisfactory transient performance, it is advisable to consider the pole clustering specifications in the controller synthesis while preserving tractability. Regional pole placement aims to place poles in a prescribed region of the left-half complex plane [19]. In practice, for the system involving uncertainties and exogenous disturbances, regional pole placement is more readily to keep the robustness than other methods of pole placement.

The LMI region in [20] is employed to deal with the constraints of regional pole placement. The disk $D(-q,\sigma)$ ($q>\sigma>0$) is chosen as the LMI region, the following theorem is applied.

Theorem 2 [11]. For each local system matrix $\boldsymbol{A}_{cli}$ in (17), the eigenvalues of each $\boldsymbol{A}_{cli}$ locate at the disk $D(-q,\sigma)$, if and only if the following LMI is satisfied.

$$\begin{bmatrix} -\sigma \boldsymbol{X} & -\sigma \boldsymbol{I} & \boldsymbol{A}_i \boldsymbol{X} + \boldsymbol{B}_u \hat{\boldsymbol{C}}_i + q\boldsymbol{X} & \boldsymbol{A}_i + \boldsymbol{B}_u \hat{\boldsymbol{D}}_i \boldsymbol{C}_y + q\boldsymbol{I} \\ * & -\sigma \boldsymbol{Y} & \hat{\boldsymbol{A}}_i + q\boldsymbol{I} & \boldsymbol{Y}\boldsymbol{A}_i + \hat{\boldsymbol{B}}_i \boldsymbol{C}_y + q\boldsymbol{Y} \\ * & * & -\sigma \boldsymbol{X} & -\sigma \boldsymbol{I} \\ * & * & * & -\sigma \boldsymbol{Y} \end{bmatrix} \prec 0 \quad (22)$$

Remark 3. Theorem 1 and 2 are derived from [11], which aim to design a dynamic output-feedback fault tolerant controller

for general T-S fuzzy systems. In this paper, we do not give the proofs of Theorem 1 and 2 for brevity.

Remark 4. With some conservatism, the multi-objective control problem is reduced to solving LMIs (19), (20), and (22), which is finally transferred to solving convex optimization problems by using the *LMI Toolbox* in Matlab.

V. Simulation Results

In this section, simulations in the Simulink-Carsim environment are conducted to validate effectiveness of the proposed compensator. The desired large-curvature path to be followed is selected as the *Half Figure 8* provided in Carsim. Fig.3 presents the relationship between road curvature and arc-length of the path. By assuming the tire-road friction coefficient μ=0.9, the maximum vehicle speed can be calculated as $V_{x\max} = \sqrt{\mu g / \rho_r} \approx 21$ m/s when negotiating the curve with consideration of the friction circle limitation [21]. In simulation, a constant vehicle speed of 16 m/s is chosen, being a typical high speed for negotiating the *Half Figure 8* with a curvature of 0.02 m^{-1}.

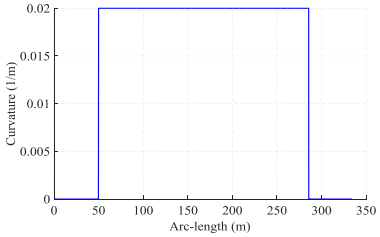

Fig.3 Relationship between road curvature and are-length

Variation range of the uncertain parameters describing the driver's characteristics can be determined as in Table III by referring to [6] [7] [15]. Two representative drivers are selected to conduct the path following maneuver, parameters of which are shown in Table IV. For both drivers, the derivative time constant τ_L and preview time T_p are assumed to be identical since these parameters show little difference in a specific scenario [6] [7].

TABLE III. VARIATION RANGE OF PREMISE VARIABLES

Parameter	K_P	K_c	τ_L	T_d	T_p
Minimum	0.80	0.50	0.10s	0.12s	0.60s
Maximum	5.00	3.00	0.34s	0.30s	2.50s

TABLE IV. DRIVERS SELECTED FOR THE TEST

Parameter	K_P	K_c	τ_L	T_d	T_p
Driver A	3.20	1.60	0.20	0.14	0.82
Driver B	2.20	1.00	0.20	0.20	0.82

Fig.4 shows the pole locations of the uncontrolled and controlled DVR systems with Driver A and B. The disk D(-15,13.5) is chosen as the LMI region for pole placement. As depicted in Fig.4, all poles locate in the disk for the controlled DVR systems, and the stabilities of both controlled systems have been greatly improved.

Fig.5 gives the *Half-Figure-8-shaped* path-following trajectories of vehicle CG with and without control for systems driven by both drivers. From Fig.5 it can be observed that both drivers cannot achieve the path-following maneuvers without the steering assistance, while the maneuvers are well completed with the steering assistance.

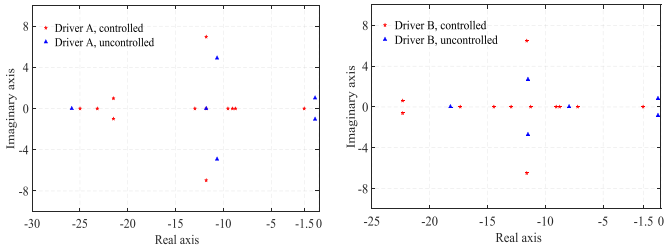

(a) (b)

Fig.4 Pole locations of the DVR system: (a) for Driver A, (b) for Driver B.

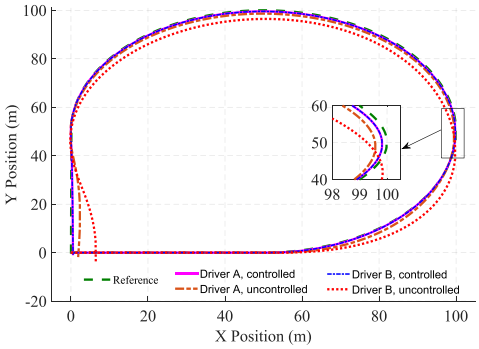

Fig.5 The half 8-shaped path following trajectories of vehicle CG

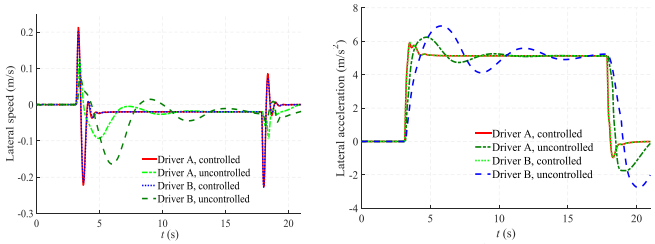

(a) (b)

Fig.6 Vehicle response of lateral speed and acceleration

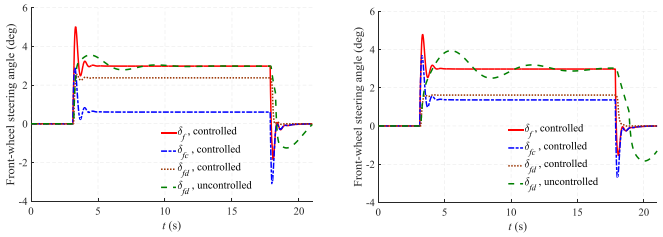

(a) (b)

Fig 7. Front-wheel steering angle: (a) for driver A, (b) for driver B

Especially in the exit segment of the curve, movements of the vehicles for both drivers with the steering assistance are corrected on the desired straight path.

Fig.6 presents the lateral speed V_y and acceleration a_y response of the vehicles. V_y is close to zero when the control is applied, which implies that the lateral stability of the vehicle is enhanced. In addition, a_y is reduced and stabilized. When the vehicle negotiates the entry and exit of the curve, there are some instantaneous oscillations for V_y, a_y, and the front-wheel steering angle, as can be observed in Fig. 7, mainly because of the sudden saltation of the road curvature as shown in Fig. 3.

The performance of path following and driver's workload can be quantified by some indexes. Similar to [13][22], the performances of path following considering vehicle's orientation and position error, driver's physical and mental workloads, and control effort of DPDC compensator, are

defined as $J_1=\int_0^\infty \left(p\psi_L^{\ 2}+q_1 y_L^{\ 2}\right)dt$, $J_2=\int_0^\infty q_2\delta_{fd}^{\ 2}\,dt$, $J_3=\int_0^\infty q_3\dot{\delta}_{fd}^{\ 2}\,dt$, $J_4=\int_0^\infty q_4\delta_{fc}^{\ 2}\,dt$, respectively, where p, q_i (i=1,2,3,4) are weights. It is obvious that a smaller J_1 indicates better performance of path following, smaller J_2 and J_3 imply less energy consumption and mental pressure of the driver, and a larger J_4 means more assistance by the compensator. Results of the performances are shown in Table V.

Table V. INDEXES FOR PATH FOLLOWING PERFORMANCE AND DRIVER'S WORKLOADS

Condition	J_1	J_2	J_3	J_4
Driver A with control	5.448	13.21	12.60	1.418
Driver A without control	103.6	21.94	15.53	--
Driver B with control	5.429	6.100	3.829	5.016
Driver B without control	593.7	23.16	6.697	--

From the index J_1 without control, we can observe that Driver A is more experienced than Driver B in the simulation scenario. In the case with control, the DPDC compensator provides the more experienced Driver A with less assistance and the less experienced driver B with more assistance. This indicates that the proposed controller can provide different human drivers with individual assistance. Furthermore, when the controller is applied, the physical and mental workloads of both drivers are greatly reduced, as can be observed with the values of J_2 and J_3.

VI. CONCLUSION AND FUTURE WORK

In this paper, fuzzy full-order dynamic output-feedback control with consideration of different human driver's characteristics is proposed for large-curvature path following. The path following model is formulated based on the two-point preview control, and a two-level driver model is built by considering the driver's compensatory and anticipatory actions. Five characteristic parameters are adopted to describe the driver's steering behavior and considered as the uncertainties for the DVR system with different drivers. The T-S fuzzy approach is applied to deal with these uncertainties, and finally design of the DPDC compensator is reduced to solving several LMIs. Simulation under Simulink-Carsim combined environment is conducted to validate effectiveness of the proposed shared steering controller. Results of the performance indexes show that the proposed compensator can provide different human drivers with individual steering assistance, as well as reduction of the driver's physical and mental workloads. Simulation results of the vehicle lateral velocity and lateral acceleration appeared with instantaneous oscillation due to saltation of the road curvature. A possible feasible solution is to introduce the measurable road curvature into the output part of the DPDC compensator (16) by bringing in another gain variable. This will be our future work.

REFERENCES

[1] A. T. Nguyen, C. Sentouh, J. C. Popieul, "Online adaptation of the authority level for shared lateral control of driver steering assist system using dynamic output feedback controller," in *Industrial Electronics Society, 41st Annual Conference of IEEE*, pp. 003767-003772, 2015.

[2] A. T. Nguyen, C. Sentouh, J. C. Popieul, "Driver-automation cooperative approach for shared steering control under multiple system constraints: Design and experiments," *IEEE Trans. on Industrial Electronics*, vol.64, pp. 3819-3830, 2017.

[3] H. Wang, H. Kong, Z. Man, Z. Cao, and W. Shen, "Sliding mode control for steer-by-wire systems with AC motors in road vehicles," *IEEE Trans. on Industrial Electronics*, vol.61, pp.1596-1611,2014.

[4] S. W. Oh, H. C. Chae, S. C. Yun, and C. S. Han, "The design of a controller for the steer-by-wire system," *JSME International Journal Mechanical Systems, Machine Elements and Manufacturing*, 47(3), 896-907, 2004.

[5] S. M. Erlien, S. Fujita, J. C Gerdes, "Shared steering control using safe envelopes for obstacle avoidance and vehicle stability," *IEEE Trans. on Intelligent Transportation Systems*, vol.17, pp.441-451, 2016.

[6] Y. W. Chai, Y. Abe, Y. Kano, and M. Abe, "A study on adaptation of SBW parameters to individual driver's steer characteristics for improved driver–vehicle system performance," *Vehicle System Dynamics*, vol.44 (sup1), pp.874-882, 2006.

[7] J. Ishio, H. Ichikawa, Y. Kano, and M. Abe, "Vehicle-handling quality evaluation through model-based driver steering behaviour,"*Vehicle System Dynamics*, vol.46 (S1), pp.549-560, 2008.

[8] A. T. Nguyen, T. Laurain, R. Palhares, J. Lauber, C. Sentouh, and J. C. Popieul, "LMI-based control synthesis of constrained Takagi–Sugeno fuzzy systems subject to L_2 or L_∞ disturbances," *Neurocomputing*, vol. 207, pp.793-804, 2016.

[9] H. Du, N. Zhang, "Fuzzy control for nonlinear uncertain electrohydraulic active suspensions with input constraint," *IEEE Trans. on Fuzzy Systems*, vol.17, pp.343-356, 2009.

[10] H. Li, J. Yu, C. Hilton, and H. Liu, "Adaptive sliding-mode control for nonlinear active suspension vehicle systems using T–S fuzzy approach," *IEEE Trans. on Industrial Electronics*, vol.60, pp.3328-3338, 2013.

[11] K. Zhang, B. Jiang, and M. Staroswiecki, "Dynamic output feedback-fault tolerant controller design for Takagi–Sugeno fuzzy systems with actuator faults," *IEEE Trans. on Fuzzy Systems*, vol.18, pp.194-201, 2010.

[12] J. Wang, M. Dai, G. Yin, and N. Chen, "Output-feedback robust control for vehicle path tracking considering different human drivers' characteristics," *Mechatronics*, 2017, to be published.

[13] J. Wang, G. Zhang, R. Wang, S. C. Schnelle, and J. Wang, "A gain-scheduling driver assistance trajectory-following algorithm considering different driver steering characteristics," *IEEE Trans. on Intelligent Transportation Systems*, vol.18, pp.1097-1108, 2017.

[14] M. Fu, "Pole placement via static output feedback is NP-hard," IEEE Trans. on Automatic Control, vol.49(5), pp.855-857, 2004.

[15] L. Saleh, P. Chevrel, F. Claveau, J. F. Lafay, and F. Mars, "Shared steering control between a driver and an automation: Stability in the presence of driver behavior uncertainty," IEEE Trans. on Intelligent Transportation Systems, vol.14, pp.974-983, 2013.

[16] M. Franck, J. Navarro, "Where we look when we drive with or without active steering wheel control," *PloS one*, 2012.

[17] C. Sentouh, P. Chevrel, F. Mars, and F. Claveau, "A sensorimotor driver model for steering control," in *Conf. IEEE Systems, Man and Cybernetics*, San Antonio, pp. 2462-2467.

[18] K. Tanaka, H. O. Wang, "Fuzzy control systems design and analysis: a linear matrix inequality approach," John Wiley & Sons, 2004.

[19] C. Mahmoud, P. Gahinet, and P. Apkarian, "Robust pole placement in LMI regions," *IEEE trans. on Automatic Control*, vol.44, pp.2257-2270, 1999.

[20] H. Zhang, X. Zhang, and J. Wang, "Robust gain-scheduling energy-to-peak control of vehicle lateral dynamics stabilization," *Vehicle System Dynamics*, vol.52, pp.309-340, 2014.

[21] J. Funke, J. C. Gerdes, "Simple clothoid lane change trajectories for automated vehicles incorporating friction constraints," *Journal of Dynamic Systems, Measurement, and Control*, vol.138, 021002, 2016.

[22] W. Wang, J. Xi, C. Liu, and X. Li, "Human-centered feed-forward control of a vehicle steering system based on a driver's path-following characteristics," *IEEE Trans. on Intelligent Transportation Systems*, vol.18(6), pp.1440-1453, 2017.